Atmos. Meas. Tech. Discuss., 5, 8539–8578, 2012
www.atmos-meas-tech-discuss.net/5/8539/2012/
doi:10.5194/amtd-5-8539-2012

Atmospheric Measurement Techniques Discussions

Improved water vapour spectroscopy in the 4174–4300 cm^{-1} region and its impact on SCIAMACHY HDO/H_2O measurements

R. A. Scheepmaker[1], C. Frankenberg[2], A. Galli[1], A. Butz[3], H. Schrijver[1], N. M. Deutscher[4,5], D. Wunch[6], T. Warneke[4], S. Fally[7], and I. Aben[1]

[1]SRON Netherlands Institute for Space Research, Utrecht, The Netherlands
[2]Jet Propulsion Laboratory, California Institute of Technology, Pasadena, CA, USA
[3]IMK-ASF, Karlsruhe Institute of Technology, Karlsruhe, Germany
[4]Institute for Environmental Physics, University of Bremen, Bremen, Germany
[5]Centre for Atmospheric Chemistry, University of Wollongong, Wollongong, Australia
[6]Department of Earth Science and Engineering, California Institute of Technology, Pasadena, CA, USA
[7]Formerly at Institut d'Aéronomie Spatiale de Belgique (IASB-BIRA), Brussels, Belgium

Received: 2 September 2012 – Accepted: 19 November 2012 – Published: 29 November 2012

Correspondence to: R. A. Scheepmaker (r.a.scheepmaker@sron.nl)

Published by Copernicus Publications on behalf of the European Geosciences Union.

Abstract

The relative abundance of the heavy water isotopologue HDO provides a deeper insight in the atmospheric hydrological cycle. The SCanning Imaging Absorption spectroMeter for Atmospheric CartograpHY (SCIAMACHY) allows global retrievals of the ratio HDO/H_2O in the 2.3 micron wavelength range. However, the spectroscopy of water lines in this region remains a large source of uncertainty for these retrievals. We therefore evaluate and improve the water spectroscopy in the range 4174–4300 cm^{-1} and test if this reduces systematic uncertainties in the SCIAMACHY retrievals of HDO/H_2O. We use a laboratory spectrum of water vapour to fit line intensity, air broadening and wavelength shift parameters. The improved spectroscopy is tested on a series of ground-based high resolution FTS spectra as well as on SCIAMACHY retrievals of H_2O and the ratio HDO/H_2O. We find that the improved spectroscopy leads to lower residuals in the FTS spectra compared to HITRAN 2008 and Jenouvrier et al. (2007) spectroscopy and the retrievals become more robust against changes in retrieval window. For both the FTS and SCIAMACHY measurements the retrieved total columns H_2O decrease by 2–4 % and we find a negative shift of the HDO/H_2O ratio, which for SCIAMACHY is partly compensated by changes in the retrieval setup and calibration software. The updated SCIAMACHY HDO/H_2O product shows somewhat steeper latitudinal and temporal gradients and a steeper Rayleigh distillation curve, strengthening previous conclusions that current isotope-enabled general circulation models underestimate the variability in the near-surface HDO/H_2O ratio.

1 Introduction

Water vapour is the strongest natural greenhouse gas, with a positive feedback on global warming (Soden et al., 2005). However, many processes related to the hydrological cycle and its response to climate change are poorly understood. To progress towards robust climate predictions, global General Circulation Models (GCMs) must

AMTD
5, 8539–8578, 2012

therefore correctly model the hydrological cycle, for which isotopes can provide a valuable benchmark.

In the study of hydrological cycles, the fractionation of stable water isotopologues, such as HDO and $H_2{}^{18}O$, has proved to be a useful proxy for evaporation and condensation temperatures (Dansgaard, 1964). This led to the application of stable water isotopologues in the field of paleoclimatology (Dansgaard et al., 1969) and in numerous studies of atmospheric transport and recycling processes (Craig and Gordon, 1965; Ehhalt, 1974; Jouzel et al., 1987; Risi et al., 2010).

Initially, most studies made use of isotope data from in-situ measurements, such as ice cores (Jouzel et al., 1997; Petit et al., 1999), aircraft flights (Ehhalt et al., 2005) or the IAEA's Global Network of Isotopes in Precipitation (the GNIP database, see, e.g. Araguás-Araguás et al., 2000). More recently, remotely-sensed measurements of the water vapour stable isotopic composition have become available, both from satellite-based instruments such as the Interferometric Monitor for Greenhouse gases (IMG, Zakharov et al., 2004), the Thermal Emission Spectrometer (TES, Worden et al., 2007), the SCanning Imaging Absorption SpectroMeter for Atmospheric CartograpHY (SCIAMACHY, Frankenberg et al., 2009) and the Infrared Atmospheric Sounding Interferometer (IASI, Herbin et al., 2009; Lacour et al., 2012), as well as from ground-based networks of Fourier-Transform Spectrometers (FTS), such as the Total Carbon Column Observing Network (TCCON, Wunch et al., 2011) and the Network for Detection of Atmospheric Composition Change (NDACC, formerly the Network for Detection of Stratospheric Change (NDSC), Kurylo and Solomon, 1990). Combined, these measurements have the potential to assess and improve the performance of current GCMs, as recently shown by Frankenberg et al. (2009); Risi et al. (2010, 2012a,b); Schneider et al. (2010b); Yoshimura et al. (2011).

Although these comparisons with the datasets are used to evaluate model performance, the datasets themselves also undergo continuous improvements and extensions. In this paper we aim to further improve the SCIAMACHY HDO/H_2O dataset by evaluating and improving the water spectroscopy used in the retrieval. Uncertainties in

AMTD
5, 8539–8578, 2012

absorption line parameters are a common source of uncertainty in the retrieval of atmospheric trace gases. Frankenberg et al. (2008a) and Schneising et al. (2009) showed that changing the water vapour spectroscopic parameters removed a tropical bias in methane retrieved with SCIAMACHY. Similarly, by systematically updating the pressure broadening parameters of methane absorption lines from 5860 to 6185 cm^{-1} using laboratory spectra, Frankenberg et al. (2008b) reduced the systematic fit residuals of high-resolution FTS measurements by a factor of 3–4 and further improved the accuracy of the low-resolution SCIAMACHY retrievals of methane by ∼ 1 % of the column averaged mixing ratio. These results were qualitatively confirmed by Schneising et al. (2009) using an independent retrieval algorithm.

Here, we apply a similar technique with the aim of reducing any possible systematic bias in retrievals of HDO/H_2O from SCIAMACHY. We use a high-resolution laboratory spectrum of a mixture of water vapour and air between 4174–4300 cm^{-1} to systematically improve the intensity, air pressure broadening and pressure shift parameters of the water lines. We then test the improved spectroscopy on a series of ground-based high-resolution FTS spectra as well as on low-resolution SCIAMACHY retrievals of H_2O and the ratio HDO/H_2O.

Throughout this work we express the ratio HDO/H_2O of the retrieved vertical column densities using the standard "delta-notation" for the fractionation of HDO relative to Vienna Standard Mean Ocean Water (VSMOW):

$$\delta D = \left(\frac{VCD(HDO)/VCD(H_2O)}{R_s} - 1 \right) \times 1000\ ‰, \quad (1)$$

in which VCD stands for the Vertical Column Density and $R_s = 3.1152 \times 10^{-4}$ is the HDO abundance of VSMOW (Craig, 1961).

We describe the setup used for improving the water spectroscopy in Sect. 2. The impact of the improved spectroscopy is discussed in Sect. 3 for the ground-based FTS retrievals and in Sect. 4 for the SCIAMACHY HDO/H_2O and H_2O retrievals. We conclude our work in Sect. 5.

AMTD
5, 8539–8578, 2012

2 Improved water spectroscopy

Jenouvrier et al. (2007) obtained a series of high-resolution FTS spectra of water vapour in a gas cell in the 4200–6600 cm^{-1} region, which they used to construct a new linelist of spectral parameters, including many new weak lines. We have used one spectrum from this series (run *j* in their Table 1) in the range 4174–4300 cm^{-1} to further update the derived line parameters. The range 4174–4300 cm^{-1} was chosen to provide overlap with the different micro windows used by the CO, H_2O and HDO/H_2O retrievals in channel 8 of SCIAMACHY. We first divided by a blank spectrum (their run *a*) to normalise the spectrum and remove any contribution from water vapour absorption between the gas cell and the spectrometer. The normalised spectrum is shown in the top panel of Fig. 1. The gas cell for run *j* contained a mixture of water vapour (a partial pressure of 4.04 hPa) and air (a partial pressure of 333.6 hPa) at a temperature of 293 K, and had an effective path length of 602.32 m, which corresponds to a total H_2O column density of 6.02×10^{21} molecule cm^{-2}. However, due to possible condensation of water vapour on the cell walls, or evaporation of water residue in the cell, the actual total column density of water vapour in the cell could differ. We therefore determined the total column density by fitting the spectrum, allowing only for a change in the column density while keeping all line parameters fixed to the Jenouvrier et al. (2007) values. This resulted in a total column density of 6.12×10^{21} molecule cm^{-2}.

We then fixed the total column density and fitted the spectrum again, using an Optimal Estimation technique that relies on additional constraints (Rodgers, 2000), similar to the technique described in Frankenberg et al. (2008b). The target parameters were the line intensity, pressure broadening coefficient (γ_{air}) and the pressure-induced shift (δ_{air}) for each individual water line, as well as a low order polynomial to allow for broadband baseline structures. For the details we refer to Frankenberg et al. (2008b). The forward model, which simulates the transmission spectrum through the gas cell, assumed a Voigt line shape.

AMTD
5, 8539–8578, 2012

The self-broadening coefficient (γ_{self}) was kept fixed at five times the pressure broadening coefficient: $\gamma_{self}/\gamma_{air} = 5$. This is consistent with the SCIAMACHY HDO/H_2O retrievals, which take self broadening into account by means of an effective pressure, for which it is also assumed that $\gamma_{self}/\gamma_{air} = 5$. Figure 2 shows the $\gamma_{self}/\gamma_{air}$ ratio from the Jenouvrier et al. (2007) spectroscopy. It highlights that the use of the fixed ratio of 5 is justified for the majority of spectral lines in the different retrieval windows under study. We tested the effect of fitting the self broadening as an additional free parameter and it leads to a maximum change of 4 ‰ on the δD retrieved from SCIAMACHY (keeping the ratio fixed to $\gamma_{self}/\gamma_{air} = 5$ for the SCIAMACHY retrieval).

The prior covariances (1σ) during the laboratory fit were 10 % for the relative intensity and 0.04 $cm^{-1}\,atm^{-1}$ for the pressure broadening coefficient and pressure shift. For H_2O lines with an intensity weaker than $10^{-25}\,cm^{-1}(molecule\,cm^{-2})^{-1}$ and HDO lines weaker than $2.7 \times 10^{-26}\,cm^{-1}(molecule\,cm^{-2})^{-1}$ the covariances of the pressure broadening and shift were $< 10^{-5}$ in order to constrain the fit of these parameters to the a priori values for the weakest lines, because they would not be well constrained. For the a priori line parameters between 4200–4300 cm^{-1} the values from Jenouvrier et al. (2007) were used. Between 4174–4200 cm^{-1} the values were taken from the HITRAN08 database (Rothman et al., 2009) because Jenouvrier et al. (2007) do not provide parameters in this range.

To reduce the uncertainty in the fitted air broadening parameters, ideally one would perform a simultaneous fit to multiple spectra taken at different air pressures (Benner, 1995). However, Jenouvrier et al. (2007) mention a variable contamination of HDO in the gas cell (relative to natural water) caused by the residue of earlier experiments with HDO enhanced water samples. Without correcting for this contamination the updated line intensities of the HDO lines would be abnormally high. We have corrected for this contamination by first fitting only for the line intensities. From the updated HDO intensities a correction factor was found, which was taken into account during the final fit of the spectrum. Because the amount of contamination was variable between the

AMTD
5, 8539–8578, 2012

different measurements, due to the pumping and filling of the cell, we had to restrict our analysis to a single spectrum.

In the bottom panels of Fig. 1 we show the improved fit residuals after the line parameters have been updated. For comparison we also show the fit residuals using the original Jenouvrier et al. (2007) and HITRAN08 line parameters. It shows that the fit residuals have been strongly reduced by updating the line parameters. It should be noted that the HITRAN08 database was compiled with an algorithm using a mixture of measurements, calculated and semi-empirical data (Rothman et al., 2009). The parameters from Jenouvrier et al. (2007) were used in this algorithm, but were not simply copied. The close-up at the bottom panel of Fig. 1 shows 4 regions where the residuals are relatively high, also for the updated line list. These residuals are caused by the edges of the micro windows used for the fitting procedure, which were deliberately chosen in regions without strong water lines. Ratios between the updated and original parameters are shown in Fig. 3. In the supplementary material with this paper we provide the full list of updated line parameters.

3 Impact on ground-based FTS H_2O retrievals

We have tested the impact of the updated water spectroscopy on a series of total column retrievals of high-resolution ground-based direct-sun FTS spectra. Due to their high resolution, improvements in the spectroscopic line parameters will show up clearly as improvements in the fit residuals (Frankenberg et al., 2008a,b), whereas a comparison with a time series of known total columns could reveal improvements in the retrieval accuracy and precision (Galli et al., 2012). To sample different latitudes and thus different total water columns, we have used measurements from FTS stations at Ny Ålesund (one spectrum, Pałm et al., 2010), Bremen (seven spectra, Messerschmidt et al., 2011) and Paramaribo (three spectra, Warneke et al., 2010), as well as two time series of 50 spectra each from Park Falls (Washenfelder et al., 2006) and Darwin (Deutscher et al., 2010). For the spectra from Park Falls and Darwin we also know the retrieved total

AMTD
5, 8539–8578, 2012

columns of H_2O that were derived in different spectral windows around 1.6 µm using the GFIT algorithm. These TCCON measurements will be used as our time series of known measurements.

3.1 Retrieval algorithm

For the retrieval algorithm we used a simplified version of the algorithm from Butz et al. (2011), also described in Galli et al. (2012). Retrieval parameters are the total column number densities of the target species H_2O and the interfering species HDO, $H_2{}^{18}O$, CO and CH_4, a second order polynomial for the baseline of the spectrum and a spectral shift. We have used a retrieval window of 4174–4300 cm^{-1} (the entire window for which the line parameters were updated) as well as a retrieval window covering 4212–4248 cm^{-1}. The latter window covers the same spectral range as the retrieval window of the SCIAMACHY HDO/H_2O measurements and allows for a more consistent comparison. The retrieval algorithm relies on prior information for the vertical profiles of pressure, humidity, temperature, CO and CH_4. For the pressure, humidity and temperature the profile was extracted from the European Centre for Medium-range Weather Forecasts (ECMWF) ERA-interim analysis. The ERA-interim fields are 6-h and on a $1.5^\circ \times 1.5^\circ$ longitude×latitude grid and were interpolated to the time and location of the FTS measurements. For the single measurement taken at Ny Ålesund a vertical profile from a radiosonde was also available. For the FTS measurements that were taken in 2007 (five of the seven Bremen spectra and all three Paramaribo spectra) the CO and CH_4 a priori profiles were taken from the Chemistry Transport Model (TM4) runs (Meirink et al., 2006) and interpolated to the time and location of the measurements. For the Ny Ålesund spectrum (from 2005) and two Bremen spectra (from 2006) these data were not available, so these profiles were interpolated to the correct location but for the corresponding day in 2007. For the Park Falls and Darwin spectra we used a local yearly averaged profile for both CH_4 and CO. We have tested

AMTD
5, 8539–8578, 2012

that changing the a priori CH_4 and CO profile from a spatially and temporally colocated profile to a globally averaged profile does not change our conclusions.

3.2 Impact on the residuals

In Fig. 4 we show the impact of the updated spectroscopy on a Paramaribo FTS spectrum taken at 11:38 UT on 27 October 2007. The spectrum shows many strong water absorption lines due to the tropical location and consequently high total water column (a fitted total water column of 1.6×10^{23} molecule cm^{-2}). The figure shows that the updated line list results in an improvement of up to $\sim 12\,\%$ (of the continuum level) in the fit residuals compared to using the water line parameters from either HITRAN08 or Jenouvrier et al. (2007). Similar improvements of fit residuals are found for all other spectra from Paramaribo, Ny Ålesund, Bremen, Park Falls and Darwin.

Although the majority of the fit residuals improved, we also find that a few specific residuals deteriorated using the updated spectroscopy. This is most noticeable around 4263.2 cm^{-1} and 4275 cm^{-1}. We show a close-up of the first residual in Fig. 5. These deteriorated residuals are likely caused by our fixed $\gamma_{self}/\gamma_{air}$ ratio of 5.0, since for these lines the ratio is actually ~ 8 (Fig. 2). The residuals of the laboratory spectrum fit (panel d in Fig. 5) are reduced with respect to the Jenouvrier et al. (2007) line list due to a small negative δ_{air} shift combined with a reduction in γ_{air}. With the fixed ratio, this reduction in γ_{air} implies a large, and possibly erroneous, reduction in γ_{self}. Moreover, the deteriorated residuals partly overlap with CH_4 lines of which the line parameters might also be inaccurate, further complicating the fit. We tested that fitting the γ_{air} and γ_{self} parameters independently on the laboratory spectrum leads to less deterioration in the residuals of the FTS fit, even if during the FTS fit γ_{self} is again fixed to $5 \times \gamma_{air}$. However, for consistency, and because the deteriorated residuals are outside the SCIAMACHY HDO/H_2O retrieval window, we decided to keep the $\gamma_{self}/\gamma_{air}$ ratio fixed for all laboratory, FTS and SCIAMACHY fits.

AMTD
5, 8539–8578, 2012

3.3 Impact on precision and accuracy

To study the impact of the updated spectroscopy on retrieval precision and accuracy (i.e. bias), we have compared the Ny Ålesund, Bremen and Paramaribo FTS retrievals with H_2O columns that we derived from the colocated ECMWF profiles. For Ny Ålesund we also have data from a colocated radiosonde, launched 188 min after the FTS measurement. We compared the Park Falls and Darwin retrievals with H_2O columns that were fitted around 1.6 µm using TCCON's GFIT algorithm (Wunch et al., 2011).

Ideally, these reference data would be independent of the spectroscopy being studied and free of any biases. The TCCON dry-air mole fractions, for example, have been calibrated with independent data from nearby sonde profiles. However, such calibrations have not been applied to the total column values that we use as our reference for the Park Falls and Darwin retrievals. Furthermore, we should note that the choice of the fixed total column density of the gas cell used for the laboratory measurements could lead to a bias. As described in Sect. 2, we have slightly increased the column density compared to the literature value, for which we first fixed the line parameters to the Jenouvrier et al. (2007) values. Any change in this column density or the initial line intensities could lead to a bias. Similarly, different methods to integrate ECMWF profiles could lead to a bias. It is therefore meaningless to study the absolute accuracy in the comparison between the total columns of our retrievals and those from our reference data. We can, however, use reference data to study the retrieval precision (i.e. measurement-to-measurement variability) and the robustness of the bias against changes in the retrieval window.

In the top panel of Fig. 6 we show the relative differences between the total column H_2O from our retrievals and the integrated ECMWF profiles. No clear improvement in the scatter (precision) can be observed for the updated line list, but there are some differences in the bias between the line lists. As mentioned above, we cannot draw conclusions on the absolute accuracy of the different line lists. We do find, however, a striking difference in the robustness of the retrievals to the change in the fitting window

AMTD
5, 8539–8578, 2012

from 4174–4300 cm^{-1} (solid lines) to 4212–4248 cm^{-1} (dashed lines). Retrievals using the updated line list are robust against this change, while retrievals using the other line lists are more sensitive to the spectral window used for the retrieval. Being robust against changes in the fitting window provides more confidence in the spectroscopy and is clearly advantageous both for current and future instrumentation, as it allows for a more flexible choice of the retrieval window.

In the bottom panel of Fig. 6 we compare δD derived from these FTS retrievals. Also here it is evident that the retrievals using the updated line list are most robust against the change in retrieval window. Although we cannot verify any possible constant bias in δD due to the lack of reference data, there is a clear correlation between δD and the total amount of moisture in the column (low for arctic Ny Ålesund and high for tropical Paramaribo), consistent with the rainout effect caused by Rayleigh distillation (Dansgaard, 1964).

In Fig. 7 (bottom panel) we show time series of the relative differences between fitted H_2O columns at 2.3 µm and the H_2O columns from TCCON's GFIT algorithm at 1.6 µm. The time series are for 50 Park Falls spectra, the results for 50 Darwin spectra look similar. The top panel shows the time series of the absolute H_2O columns. The overall correlation between the 1.6 µm and 2.3 µm region is very good (Pearson's $R = 0.999$ for all line lists).

From the Park Falls and Darwin time series we derived different statistics, which are summarised in Table 1 for the three different line lists and the two different retrieval windows. The precision of the retrievals is defined as the standard deviation σ around the mean relative difference with the TCCON values. The median of the relative differences is representative of the bias and the fit residuals are expressed as the averaged reduced chi-square: $\langle \chi^2/\nu \rangle$. Figure 7 and Table 1 show that there is no improvement in precision for the updated line list: all σ's are comparable (the small differences could be explained by the average relative error of the TCCON values: 0.45 % for Darwin and 0.73 % for Park Falls). Our updated line list, however, shows a clear reduction in $\langle \chi^2/\nu \rangle$ compared to the other line lists and the median is more robust against the change in

AMTD
5, 8539–8578, 2012

retrieval window. Similar to Fig. 6, this robustness is also visible in the lower panel of Fig. 7 as the difference between the solid and dashed lines is smallest for the updated line list.

4 Impact on SCIAMACHY retrievals

In the previous section we saw the impact of the updated spectroscopy on high-resolution ground-based FTIR measurements. Besides lower fit residuals and increased robustness against a fit window change, the updated spectroscopy led to lower total H_2O columns and a negative shift in δD compared to the original Jenouvrier et al. (2007) line list. Although we have tested that these results do not change if we convolve the high-resolution TCCON spectra to the lower resolution of SCIAMACHY, in this section we study the impact on the SCIAMACHY HDO/H_2O ratio and H_2O retrievals themselves.

4.1 Retrieval algorithms

4.1.1 IMAP HDO/H_2O

The primary goal of the work presented here is to further improve the accuracy of the HDO/H_2O product retrieved from SCIAMACHY data using the Iterative Maximum A-Posteriori (IMAP) algorithm. This retrieval algorithm follows the approach from Rodgers (2000) and is almost identical to the algorithm used for SCIAMACHY's IMAP CH_4 retrievals (Frankenberg et al., 2005, 2011). We refer the reader to those papers for a more detailed description of the algorithm. The HDO/H_2O product was first described by Frankenberg et al. (2009), and consequently used in some first comparisons with isotope-enabled GCMs (Risi et al., 2010; Yoshimura et al., 2011), as well as in diverse case studies regarding, e.g. paleoclimatology using isotopic fractionation in leaf wax from lake Malawi (Konecky et al., 2011), the identification of moisture sources during

AMTD
5, 8539–8578, 2012

the Madden-Julian oscillation (Berkelhammer et al., 2012) and asian monsoon hydrology (Lee et al., 2012).

For the retrieval of the HDO/H_2O ratio we use a micro-window in channel 8 (the short-wave infrared) of SCIAMACHY, ranging from 4212 to 4248 cm^{-1}. Because SCIAMACHY observes sunlight backscattered off the Earth's surface, the radiation passes the entire atmosphere twice, resulting in strong absorption signatures of H_2O and CH_4 and weaker absorption signatures of HDO and CO. Due to this combination of wavelength range and observation geometry, we obtain a high sensitivity to water vapour near the surface, as opposed to thermal emission spectrometers such as TES and IASI, which have a peak sensitivity around ~ 700 hPa (Worden et al., 2006).

The water spectroscopy used for the original HDO/H_2O product was taken from Jenouvrier et al. (2007). The CH_4 spectroscopy was taken from the HITRAN06 database (Rothman et al., 2005, same as HITRAN08 for this region), patched with updated broadening parameters from Predoi-Cross et al. (2006). The CO spectroscopy comes from HITRAN08.

Although the effects of scattering in the atmosphere are low in the short-wave infrared, compared to shorter wavelength regions, the retrieval of absolute total columns could in principle still be biased by light-path modifications due to scattering, which are unaccounted for in the retrieval. However, these scattering effects and possibly other, unresolved instrumental biases, will mostly cancel out by strictly considering only the ratio of the retrieved total columns. This is especially true for the HDO/H_2O ratio considered here, since the applied micro-window is the same for both absorbing species, negating most wavelength dependent biases.

We use a slightly updated version of the HDO/H_2O product compared to the product described in Frankenberg et al. (2009). Before updating the water line parameters as described in Sect. 2, we fixed a bug in our temperature correction of the water line intensities from the Jenouvrier et al. (2007) temperature (293 K) to the standard reference temperature of 296 K as used by HITRAN. This resulted in 1–1.5 % lower intensities and, correspondingly, 1–1.5 % higher total column densities. Next, we included $H_2{}^{18}O$

AMTD
5, 8539–8578, 2012

as an independent third water isotopologue in the retrieval. The majority of the $H_2{}^{18}O$ lines are weaker than the HDO lines in our retrieval window. However, we found a significant (11 %) improvement in the fit residual around 4235.5 cm^{-1} of ground-based FTS spectra by including $H_2{}^{18}O$ as an independent species. Finally, we used an updated version of the SCIAMACHY instrument calibration software (the *nadc_tools* software package developed at SRON[1]), which contains many small improvements in, e.g. the orbital variation of the dark current correction. All these updates lead to small differences in the retrieved HDO/H_2O, even before updates in the spectroscopy were considered. In the remainder of this work we will indicate whether the impacts on the SCIAMACHY HDO/H_2O retrievals are caused by spectroscopic updates or by the updates to the calibration software.

4.1.2 IMLM H_2O

We also use the H_2O product retrieved in channel 8 of SCIAMACHY using the Iterative Maximum-Likelihood Method (IMLM) retrieval algorithm of Schrijver et al. (2009). This product differs from the IMAP HDO/H_2O product mainly because it is a total column product instead of a ratio product. This product has been described in detail and has been validated against total H_2O columns from ECMWF in Schrijver et al. (2009). The retrieval window used ranged from 4223 to 4250 cm^{-1}, which is slightly smaller but strongly overlapping with the window used for the HDO/H_2O ratio product (4212 to 4248 cm^{-1}).

Similarly to the original IMAP HDO/H_2O product, the water spectroscopy line list for the IMLM H_2O product was taken from Jenouvrier et al. (2007). We can therefore use this product as an additional test of the impact of the spectroscopic improvements.

[1] http://www.sron.nl/~richardh/SciaDC/

AMTD
5, 8539–8578, 2012

4.2 Impact on IMAP HDO/H_2O

First we look at the impact on the measured vertical column densities (VCDs) of H_2O and HDO of individual ground pixels using the IMAP algorithm. In Fig. 8 we show the ratio of the new VCD over the original VCD as a function of the measured slant column density (which is the more directly measured quantity than the VCD) for June 2003. The figure shows that the updated spectroscopy leads to a reduction in the H_2O VCD of ∼ 2–5 % for the majority of the ground pixels and a reduction of ∼ 4–10 % for the HDO VCD. The reduction of HDO is larger than the reduction of H_2O, which leads to a corresponding negative shift in δD of ∼ 20–50 ‰. This is consistent with the ground-based FTIR results from the previous section, where similar reductions were found for the 4212–4248 cm^{-1} retrieval window (see, e.g. the differences between the blue and red dashed lines in Fig. 6). Figure 8 also shows that the reductions are largest for the driest columns, which will have an impact on the latitudinal gradient, seasonality and Rayleigh distillation curve, as we will discuss below.

As mentioned in Sect. 4.1.1, our updated SCIAMACHY HDO/H_2O product also incorporates other updates besides the spectroscopy, such as improvements in the instrument calibration software and the inclusion of $H_2{}^{18}O$ as a separate species. Now that we have seen the impact of the updated spectroscopy, we continue with a sensititvity study to test how the dataset of Frankenberg et al. (2009) will change if we incorporate all improvements simultaneously.

In Fig. 9 we show the impact on the 2003–2005 averaged world map of δD. The top left panel shows the world map including all updates. The differences with the original world map are shown in the top right panel. The updated world map shows higher values around the tropics and lower values towards the poles. The lower panels show that this increased latitudinal gradient is caused by the combination of increased values due to the updated calibration and decreased values due to the updated spectroscopy, both already containing a small latitudinal gradient. In Fig. 10 the latitudinal gradient is shown by binning over all longitudes in four degree latitude bins. Comparisons between

AMTD
5, 8539–8578, 2012

modelled latitudinal isotope gradients and SCIAMACHY observations indicate that the Isotopes-incorporated Global Spectral Model (isoGSM) underestimates the gradient (Yoshimura et al., 2011). This underestimation becomes larger with our updated δD dataset.

Comparing the 2003–2005 averaged observed SCIAMACHY seasonality of δD in the Sahel with models, it was found that both the IsoGSM model (Frankenberg et al., 2009) and the Laboratoire de Météorologie Dynamique-Zoom (LMDZ) model (Risi et al., 2010) underestimate this seasonality. In Fig. 11 we show the impact of the updated retrieval on the Sahelian seasonality. Also here, the negative shift is largest for the driest columns, which leads to a steeper gradient. This further strengthens the previous conclusions that the models currently underestimate the seasonality relative to SCIAMACHY.

We have also tested the impact of the updated retrievals on the slope of a Rayleigh-type curve. Traditionally, a Rayleigh curve shows the relation between the amount of depletion of a water sample (expressed as the ratio HDO/H_2O) and the remaining amount of water in the sample, while the sample is subjected to either evaporation or condensation (Dansgaard, 1964). By taking the natural logarithm of these quantities, the curve becomes a straight line with a slope equal to the fractionation factor $\alpha - 1$ (a quantity that is also known as the *fractionation*). This fractionation factor α is temperature dependent and is defined as

$$\alpha = \frac{R_L}{R_V}, \tag{2}$$

where

$$R = \frac{[HDO]}{[H_2O]} \tag{3}$$

is the abundance ratio and the subscripts "L" and "V" refer to the liquid and vapour phase, respectively.

AMTD
5, 8539–8578, 2012

The temperature dependence of α has been measured (e.g. Majoube, 1971), which means that we can derive the corresponding fractionation temperature from the fitted slope of a Rayleigh-type curve. The fractionation temperature represents the average temperature of the various evaporation and condensation processes that have occured during the history of the water sample. In Fig. 12 we show a Rayleigh-type plot for the original and updated SCIAMACHY retrievals above the Sahel region (15°–23° N and 0°–10° E). For this figure we matched the IMAP HDO/H_2O retrievals on the y-axis with the IMLM H_2O retrievals on the x-axis. Monthly averages were taken from the years 2003–2005 (every monthly datapoint containing data from three years). Fitting the slopes with a linear regression, we find that for the updated retrievals the slope increases from 0.089 ± 0.014 to 0.119 ± 0.013, corresponding to a decrease in fractionation temperature from 285 ± 10 K to 266 ± 7 K. The correlation coefficient increases from 0.90 to 0.95.

Previous comparisons between the isoGSM and LMDZ models and SCIAMACHY measurements have shown that the models generally underestimate the slope of the Rayleigh-type curve. With the increased slope of our updated retrievals this underestimation further increases, underlining that a measurement bias is an unlikely explanation for the discrepancy.

4.3 Impact on IMLM H_2O

In Fig. 8 we saw that the updated spectroscopy led to a reduction of 2–5 % in the fitted H_2O VCD using the IMAP HDO/H_2O retrieval. In Fig. 13 we confirm that similar reductions are found using the IMLM H_2O retrieval. Also here, the largest relative reductions are found for the driest columns. The original IMLM H_2O columns were compared to colocated ECMWF H_2O columns by Schrijver et al. (2009), who found very good agreement, represented by slopes of the regression lines between IMLM and ECMWF in the range of 0.90–1.03. The reductions we find lower these slopes by about 0.03, which means that there remains a very good agreement between H_2O columns from IMLM and ECMWF.

AMTD
5, 8539–8578, 2012

5 Conclusions

We have updated the spectroscopic line parameters of the water molecule in the 4174 to 4300 cm^{-1} range. This range covers the windows used for the retrieval of H_2O and the ratio HDO/H_2O by the SCIAMACHY instrument onboard ENVISAT. Taking the line parameters from Jenouvrier et al. (2007) as our a priori, we applied a nonlinear constrained least squares technique based on Optimal Estimation to derive line intensities, pressure shifts and pressure broadening parameters by fitting a laboratory spectrum of water vapour. The full list of updated line parameters is provided in the supplementary material with this paper. The impact of the updated line parameters was tested on ground-based FTS measurements as well as on SCIAMACHY retrievals of the ratio HDO/H_2O and H_2O.

We find that the updated water line parameters generally lead to improved residuals in the FTS spectra. A comparison with the total column H_2O product from the TCCON stations at Park Falls and Darwin, as well FTS retrievals for stations at Ny Ålesund, Bremen and Paramaribo shows that the updated parameters make retrievals more robust against a change in the spectral window used. The retrieved total columns of H_2O decrease by 2–5 %, which is consistent with a similar decrease in total column H_2O from the lower resolution SCIAMACHY measurements. Because the decrease is stronger for total column HDO, the updated spectroscopy leads to a negative shift in the measured δD, for both FTS as well as SCIAMACHY retrievals and this shift increases for drier columns.

We have also applied other small improvements to the SCIAMACHY retrievals of the HDO/H_2O ratio, such as the inclusion of $H_2{}^{18}O$ as an additional absorbing species, and using an updated calibration software package that includes, e.g. a better characterisation of the orbital variation of the dark current. Contrary to the spectroscopy updates, these updates lead to a positive shift in δD.

The main purpose of this study was to test if further improvements to the water spectroscopy around the 4200 cm^{-1} range would lead to further improvements in the

AMTD
5, 8539–8578, 2012

SCIAMACHY retrievals of HDO/H_2O and whether spectroscopic uncertainties could even explain the previously observed model-measurement mismatch. We find that all updates in spectroscopy and instrument calibration combined have a small impact on the previous SCIAMACHY HDO/H_2O dataset first described by Frankenberg et al. (2009). The global latitudinal gradient of δD becomes steeper, as well as the δD seasonality above the Sahel, which shows even more depletion of δD in winter. This implies that the conclusions of previous studies that compared SCIAMACHY's δD measurements to modelled values still hold, namely that the current isotope-enabled GCM models underestimate the variability in near-surface δD (Frankenberg et al., 2009; Risi et al., 2010; Yoshimura et al., 2011). Plotted as a Rayleigh-type fractionation curve, the updates lead to an increase in the slope of 0.03, which corresponds to a decrease in the derived fractionation temperature of 19 K.

A detailed validation study has to be performed to judge the significance of the impact for the SCIAMACHY HDO/H_2O retrievals. For such a validation study an increasing amount of well-calibrated, ground-based FTS data of the column-averaged HDO/H_2O ratio become available (e.g. Schneider et al., 2010a; Schneider et al., 2012). This validation will be part of future work and should give us a better handle on the quality of the SCIAMACHY HDO/H_2O data.

Eventhough our updated spectroscopy is a clear improvement and results in smaller fit residuals and increased robustness against a fit window change for ground-based retrievals, further improvements of the water line parameters are possible around the 4200 cm^{-1} range. Due to the contamination in the gas cell, for example, we used a limited setup of only a single laboratory spectrum. A close collaboration between the laboratory community and the satellite community is important for further improvements, as is shown by the necessity of even better water spectroscopy for the retrieval of total column CO from the future TROPOMI instrument on ESA's Sentinel-5 Precursor mission (Galli et al., 2012).

AMTD
5, 8539–8578, 2012

Supplementary material related to this article is available online at: http://www.atmos-meas-tech-discuss.net/5/8539/2012/amtd-5-8539-2012-supplement.zip.

Acknowledgements. This researched was funded by the Netherlands Space Office as part of the User Support Programme Space Research under project GO-AO/16. AB is funded through the Emmy-Noether programme of Deutsche Forschungsgemeinschaft (DFG) through grant BU2599/1-1 (RemoteC). SF is funded by the Belgian Federal Science Policy Office, the Fonds National de la Recherche Scientifique (FNRS, Belgium) and the European Space Agency (ESA-Prodex program). US funding for TCCON comes from NASA's Terrestrial Ecology Program, grant number NNX11AG01G, the Orbiting Carbon Observatory Program, the Atmospheric CO2 Observations from Space (ACOS) Program and the DOE/ARM Program. The Darwin TCCON site was built at Caltech with funding from the OCO project, and is operated by the University of Wollongong, with travel funds for maintenance and equipment costs funded by the OCO-2 project. We acknowledge funding to support Darwin from the Australian Research Council, Projects LE0668470, DP0879468, DP110103118 and LP0562346. We further acknowledge David Griffith and Ronald Macatangay for providing the Darwin TCCON spectra and data. We acknowledge the Alfred Wegener Institute for Polar and Marine research (AWI) for providing the measurement infrastructure at Ny Ålesund and Cor Becker and his team from the Meteorological Service of Suriname for their support for the measurements at Paramaribo (Suriname). ECMWF ERA-Interim data used in this study have been obtained from the ECMWF data server. We thank Richard van Hees for his work on the *nadc_tools* software package and Pieter van der Meer for his efforts to keep the SRON cluster running.

References

Araguás-Araguás, L., Froehlich, K., and Rozanski, K.: Deuterium and oxygen18 isotope composition of precipitation and atmospheric moisture, Hydrol. Process., 14, 1341–1355, 2000. 8541

Benner, D.: A multispectrum nonlinear least squares fitting technique, J. Quant. Spectrosc. Ra., 53, 705–721, doi:10.1016/0022-4073(95)00015-D, 1995. 8544

AMTD

5, 8539–8578, 2012

Berkelhammer, M., Risi, C., Kurita, N., and Noone, D. C.: The moisture source sequence for the Madden-Julian Oscillation as derived from satellite retrievals of HDO and H_2O, J. Geophys. Res., 117, D03106, doi:10.1029/2011JD016803, 2012. 8551

Butz, A., Guerlet, S., Hasekamp, O., Schepers, D., Galli, A., Aben, I., Frankenberg, C., Hartmann, J.-M., Tran, H., Kuze, A., Keppel-Aleks, G., Toon, G., Wunch, D., Wennberg, P., Deutscher, N., Griffith, D., Macatangay, R., Messerschmidt, J., Notholt, J., and Warneke, T.: Toward accurate CO_2 and CH_4 observations from GOSAT, Geophys. Res. Lett., 38, L14812, doi:10.1029/2011GL047888, 2011. 8546

Craig, H.: Standard for reporting concentrations of deuterium and oxygen-18 in natural waters, Science, 133, 1833–1834, doi:10.1126/science.133.3467.1833, 1961. 8542

Craig, H. and Gordon, L.: Deuterium and oxygen 18 variations in the ocean and the marine atmosphere, Consiglio nazionale delle richerche, Laboratorio de Geologia Nucleare, 1965. 8541

Dansgaard, W.: Stable isotopes in precipitation, Tellus, 16, 436–468, 1964. 8541, 8549, 8554

Dansgaard, W., Johnsen, S. J., Møller, J., and Langway, C. C.: One thousand centuries of climatic record from camp century on the Greenland Ice Sheet, Science, 166, 377–380, doi:10.1126/science.166.3903.377, 1969. 8541

Deutscher, N. M., Griffith, D. W. T., Bryant, G. W., Wennberg, P. O., Toon, G. C., Washenfelder, R. A., Keppel-Aleks, G., Wunch, D., Yavin, Y., Allen, N. T., Blavier, J.-F., Jiménez, R., Daube, B. C., Bright, A. V., Matross, D. M., Wofsy, S. C., and Park, S.: Total column CO_2 measurements at Darwin, Australia – site description and calibration against in situ aircraft profiles, Atmos. Meas. Tech., 3, 947–958, doi:10.5194/amt-3-947-2010, 2010. 8545

Ehhalt, D. H.: Vertical profiles of HTO, HDO, and H_2O in the troposphere, NCAR Tech. Note NCAR-TN-STR-100, 1974. 8541

Ehhalt, D. H., Rohrer, F., and Fried, A.: Vertical profiles of HDO/H_2O in the troposphere, J. Geophys. Res., 110, 13301, doi:10.1029/2004JD005569, 2005. 8541

Frankenberg, C., Platt, U., and Wagner, T.: Iterative maximum a posteriori (IMAP)-DOAS for retrieval of strongly absorbing trace gases: Model studies for CH4 and CO_2 retrieval from near infrared spectra of SCIAMACHY onboard ENVISAT, Atmos. Chem. Phys., 5, 9–22, doi:10.5194/acp-5-9-2005, 2005. 8550

Frankenberg, C., Bergamaschi, P., Butz, A., Houweling, S., Meirink, J. F., Notholt, J., Petersen, A. K., Schrijver, H., Warneke, T., and Aben, I.: Tropical methane emissions:

AMTD
5, 8539–8578, 2012

a revised view from SCIAMACHY onboard ENVISAT, Geophys. Res. Lett., 35, 15811, doi:10.1029/2008GL034300, 2008a. 8542, 8545

Frankenberg, C., Warneke, T., Butz, A., Aben, I., Hase, F., Spietz, P., and Brown, L. R.: Pressure broadening in the $2\nu_3$ band of methane and its implication on atmospheric retrievals, Atmos. Chem. Phys., 8, 5061–5075, doi:10.5194/acp-8-5061-2008, 2008b. 8542, 8543, 8545

Frankenberg, C., Yoshimura, K., Warneke, T., Aben, I., Butz, A., Deutscher, N., Griffith, D., Hase, F., Notholt, J., Schneider, M., Schrijver, H., and Röckmann, T.: Dynamic processes governing lower-tropospheric HDO/H_2O ratios as observed from space and ground, Science, 325, 1374–1377, doi:10.1126/science.1173791, 2009. 8541, 8550, 8551, 8553, 8554, 8557, 8574, 8575, 8576

Frankenberg, C., Aben, I., Bergamaschi, P., Dlugokencky, E. J., van Hees, R., Houweling, S., van der Meer, P., Snel, R., and Tol, P.: Global column-averaged methane mixing ratios from 2003 to 2009 as derived from SCIAMACHY: trends and variability, J. Geophys. Res.-Atmos., 116, 4302, doi:10.1029/2010JD014849, 2011. 8550

Galli, A., Butz, A., Scheepmaker, R. A., Hasekamp, O., Landgraf, J., Tol, P., Wunch, D., Deutscher, N. M., Toon, G. C., Wennberg, P. O., Griffith, D. W. T., and Aben, I.: CH_4, CO, and H_2O spectroscopy for the Sentinel-5 Precursor mission: an assessment with the Total Carbon Column Observing Network measurements, Atmos. Meas. Tech., 5, 1387–1398, doi:10.5194/amt-5-1387-2012, 2012. 8545, 8546, 8557

Herbin, H., Hurtmans, D., Clerbaux, C., Clarisse, L., and Coheur, P.-F.: $H_2{}^{16}O$ and HDO measurements with IASI/MetOp, Atmos. Chem. Phys., 9, 9433–9447, doi:10.5194/acp-9-9433-2009, 2009. 8541

Jenouvrier, A., Daumont, L., Régalia-Jarlot, L., Tyuterev, V. G., Carleer, M., Vandaele, A. C., Mikhailenko, S., and Fally, S.: Fourier transform measurements of water vapor line parameters in the 4200–6600 cm^{-1} region, J. Quant. Spectrosc. Ra., 105, 326–355, doi:10.1016/j.jqsrt.2006.11.007, 2007. 8540, 8543, 8544, 8545, 8547, 8548, 8550, 8551, 8552, 8556, 8565, 8566, 8567, 8569, 8578

Jouzel, J., Russell, G. L., Suozzo, R. J., Koster, R. D., White, J. W. C., and Broecker, W. S.: Simulations of the HDO and $H_2{}^{18}O$ atmospheric cycles using the NASA/GISS general circulation model: The seasonal cycle for present-day conditions, J. Geophys. Res., 92, 14739–14760, doi:10.1029/JD092iD12p14739, 1987. 8541

Jouzel, J., Alley, R. B., Cuffey, K. M., Dansgaard, W., Grootes, P., Hoffmann, G., Johnsen, S. J., Koster, R. D., Peel, D., Shuman, C. A., Stievenard, M., Stuiver, M., and White, J.: Validity of

AMTD
5, 8539–8578, 2012

the temperature reconstruction from water isotopes in ice cores, J. Geophys. Res., 102, 26471–26488, doi:10.1029/97JC01283, 1997. 8541

Konecky, B. L., Russell, J. M., Johnson, T. C., Brown, E. T., Berke, M. A., Werne, J. P., and Huang, Y.: Atmospheric circulation patterns during late Pleistocene climate changes at Lake Malawi, Africa, Earth Planet Sc. Lett., 312, 318–326, doi:10.1016/j.epsl.2011.10.020, 2011. 8550

Kurylo, M. and Solomon, S.: Network for the Detection of Stratospheric Change: A Status and Implementation Report, NASA, Upper Atmosphere Research Program and NOAA Climate and Global Change Program, Washington DC, 1990. 8541

Lacour, J.-L., Risi, C., Clarisse, L., Bony, S., Hurtmans, D., Clerbaux, C., and Coheur, P.-F.: Mid-tropospheric δD observations from IASI/MetOp at high spatial and temporal resolution, Atmos. Chem. Phys., 12, 10817–10832, doi:10.5194/acp-12-10817-2012, 2012. 8541

Lee, J.-E., Risi, C., Fung, I., Worden, J., Scheepmaker, R. A., Lintner, B., and Frankenberg, C.: Asian monsoon hydrometeorology from TES and SCIAMACHY water vapor isotope measurements and LMDZ simulations: implications for speleothem climate record interpretation, J. Geophys. Res., 117, D15112, doi:10.1029/2011JD017133, 2012. 8551

Majoube, M.: Fractionnement en oxygène 18 et en deutérium entre l'eau et sa vapeur, J. Chim. Phys., 68, 1423–1436, 1971. 8555

Meirink, J. F., Eskes, H. J., and Goede, A. P. H.: Sensitivity analysis of methane emissions derived from SCIAMACHY observations through inverse modelling, Atmos. Chem. Phys., 6, 1275–1292, doi:10.5194/acp-6-1275-2006, 2006. 8546

Messerschmidt, J., Macatangay, R., Notholt, J., Petri, C., Warneke, T., and Weinzierl, C.: Side by side measurements of CO_2 by ground-based Fourier transform spectrometry (FTS), Tellus B, 62, doi:10.1111/j.1600-0889.2010.00491.x, 2011. 8545

Pałm, M., Melsheimer, C., Noël, S., Heise, S., Notholt, J., Burrows, J., and Schrems, O.: Integrated water vapor above Ny Ålesund, Spitsbergen: a multi-sensor intercomparison, Atmos. Chem. Phys., 10, 1215–1226, doi:10.5194/acp-10-1215-2010, 2010. 8545

Petit, J. R., Jouzel, J., Raynaud, D., Barkov, N. I., Barnola, J.-M., Basile, I., Bender, M., Chappellaz, J., Davis, M., Delaygue, G., Delmotte, M., Kotlyakov, V. M., Legrand, M., Lipenkov, V. Y., Lorius, C., Pépin, L., Ritz, C., Saltzman, E., and Stievenard, M.: Climate and atmospheric history of the past 420 000 years from the Vostok ice core, Antarctica, Nature, 399, 429–436, doi:10.1038/20859, 1999. 8541

AMTD

5, 8539–8578, 2012

Predoi-Cross, A., Brawley-Tremblay, M., Brown, L. R., Devi, V. M., and Benner, D. C.: Multi-spectrum analysis of $^{12}CH_4$ from 4100 to 4635 cm^{-1}: II. Air-broadening coefficients (widths and shifts), J. Mol. Spectrosc., 236, 201–215, doi:10.1016/j.jms.2006.01.013, 2006. 8551

Risi, C., Bony, S., Vimeux, F., Frankenberg, C., Noone, D., and Worden, J.: Understanding the Sahelian water budget through the isotopic composition of water vapor and precipitation, J. Geophys. Res., 115, D24110, doi:10.1029/2010JD014690, 2010. 8541, 8550, 8554, 8557

Risi, C., Noone, D., Worden, J., Frankenberg, C., Stiller, G., Kiefer, M., Funke, B., Walker, K., Bernath, P., Schneider, M., Bony, S., Lee, J., Brown, D., and Sturm, C.: Process-evaluation of tropospheric humidity simulated by general circulation models using water vapor isotopic observations: 2. Using isotopic diagnostics to understand the mid and upper tropospheric moist bias in the tropics and subtropics, J. Geophys. Res.-Atmos., 117, D05304, doi:10.1029/2011JD016623, 2012a. 8541

Risi, C., Noone, D., Worden, J., Frankenberg, C., Stiller, G., Kiefer, M., Funke, B., Walker, K., Bernath, P., Schneider, M., Wunch, D., Sherlock, V., Deutscher, N., Griffith, D., Wennberg, P. O., Strong, K., Smale, D., Mahieu, E., Barthlott, S., Hase, F., García, O., Notholt, J., Warneke, T., Toon, G., Sayres, D., Bony, S., Lee, J., Brown, D., Uemura, R., and Sturm, C.: Process-evaluation of tropospheric humidity simulated by general circulation models using water vapor isotopologues: 1. Comparison between models and observations, J. Geophys. Res.-Atmos., 117, D05303, doi:10.1029/2011JD016621, 2012b. 8541

Rodgers, C. D.: Inverse Methods for Atmospheric Sounding, World Scientific, Singapore, 2000. 8543, 8550

Rothman, L. S., Jacquemart, D., Barbe, A., Benner, D. C., Birk, M., Brown, L. R., Carleer, M. R., Chackerian, C., Chance, K., Coudert, L. H., Dana, V., Devi, V. M., Flaud, J., Gamache, R. R., Goldman, A., Hartmann, J., Jucks, K. W., Maki, A. G., Mandin, J., Massie, S. T., Orphal, J., Perrin, A., Rinsland, C. P., Smith, M. A. H., Tennyson, J., Tolchenov, R. N., Toth, R. A., Vander Auwera, J., Varanasi, P., and Wagner, G.: The HITRAN 2004 molecular spectroscopic database, J. Quant. Spectrosc. Ra., 96, 139–204, doi:10.1016/j.jqsrt.2004.10.008, 2005. 8551

Rothman, L. S., Gordon, I. E., Barbe, A., Benner, D. C., Bernath, P. F., Birk, M., Boudon, V., Brown, L. R., Campargue, A., Champion, J.-P., Chance, K., Coudert, L. H., Dana, V., Devi, V. M., Fally, S., Flaud, J.-M., Gamache, R. R., Goldman, A., Jacquemart, D., Kleiner, I., Lacome, N., Lafferty, W. J., Mandin, J.-Y., Massie, S. T., Mikhailenko, S. N., Miller, C. E., Moazzen-Ahmadi, N., Naumenko, O. V., Nikitin, A. V., Orphal, J., Perevalov, V. I., Perrin, A.,

AMTD
5, 8539–8578, 2012

Predoi-Cross, A., Rinsland, C. P., Rotger, M., Šimečková, M., Smith, M. A. H., Sung, K., Tashkun, S. A., Tennyson, J., Toth, R. A., Vandaele, A. C., and Vander Auwera, J.: The HITRAN 2008 molecular spectroscopic database, J. Quant. Spectrosc. Ra., 110, 533–572, doi:10.1016/j.jqsrt.2009.02.013, 2009. 8544, 8545

Schneider, M., Toon, G. C., Blavier, J.-F., Hase, F., Leblanc, T., and Gutman, S.: H_2O and δD profiles remotely-sensed from ground in different spectral infrared regions, Atmos. Meas. Tech., 3, 1599–1613, doi:10.5194/amt-3-1599-2010, 2010a. 8557

Schneider, M., Yoshimura, K., Hase, F., and Blumenstock, T.: The ground-based FTIR network's potential for investigating the atmospheric water cycle, Atmos. Chem. Phys., 10, 3427–3442, doi:10.5194/acp-10-3427-2010, 2010b. 8541

Schneider, M., Barthlott, S., Hase, F., González, Y., Yoshimura, K., García, O. E., Sepúlveda, E., Gomez-Pelaez, A., Gisi, M., Kohlhepp, R., Dohe, S., Blumenstock, T., Strong, K., Weaver, D., Pałm, M., Deutscher, N. M., Warneke, T., Notholt, J., Lejeune, B., Demoulin, P., Jones, N., Griffith, D. W. T., Smale, D., and Robinson, J.: Ground-based remote sensing of tropospheric water vapour isotopologues within the project MUSICA, Atmos. Meas. Tech. Disc., 5, 5357–5418, doi:10.5194/amtd-5-5357-2012, 2012. 8557

Schneising, O., Buchwitz, M., Burrows, J. P., Bovensmann, H., Bergamaschi, P., and Peters, W.: Three years of greenhouse gas column-averaged dry air mole fractions retrieved from satellite – Part 2: Methane, Atmos. Chem. Phys., 9, 443–465, doi:10.5194/acp-9-443-2009, 2009. 8542

Schrijver, H., Gloudemans, A. M. S., Frankenberg, C., and Aben, I.: Water vapour total columns from SCIAMACHY spectra in the 2.36 µm window, Atmos. Meas. Tech., 2, 561–571, doi:10.5194/amt-2-561-2009, 2009. 8552, 8555, 8577

Soden, B. J., Jackson, D. L., Ramaswamy, V., Schwarzkopf, M. D., and Huang, X.: The radiative signature of upper tropospheric moistening, Science, 310, 841–844, doi:10.1126/science.1115602, 2005. 8540

Warneke, T., Petersen, A. K., Gerbig, C., Jordan, A., Rödenbeck, C., Rothe, M., Macatangay, R., Notholt, J., and Schrems, O.: Co-located column and in situ measurements of CO_2 in the tropics compared with model simulations, Atmos. Chem. Phys., 10, 5593–5599, doi:10.5194/acp-10-5593-2010, 2010. 8545

Washenfelder, R. A., Toon, G. C., Blavier, J.-F., Yang, Z., Allen, N. T., Wennberg, P. O., Vay, S. A., Matross, D. M., and Daube, B. C.: Carbon dioxide column abundances at the Wis-

AMTD
5, 8539–8578, 2012

consin Tall Tower site, J. Geophys. Res., 111, D22305, doi:10.1029/2006JD007154, 2006. 8545

Worden, J., Bowman, K., Noone, D., Beer, R., Clough, S., Eldering, A., Fisher, B., Goldman, A., Gunson, M., and Herman, R.: Tropospheric Emission Spectrometer observations of the tropospheric HDO/H_2O ratio: estimation approach and characterization, J. Geophys. Res., 111, D16309, doi:10.1029/2005JD006606, 2006. 8551

Worden, J., Noone, D., Bowman, K., Beer, R., Eldering, A., Fisher, B., Gunson, M., Goldman, A., Herman, R., Kulawik, S. S., Lampel, M., Osterman, G., Rinsland, C., Rodgers, C., Sander, S., Shephard, M., Webster, C. R., and Worden, H.: Importance of rain evaporation and continental convection in the tropical water cycle, Nature, 445, 528–532, doi:10.1038/nature05508, 2007. 8541

Wunch, D., Toon, G. C., Blavier, J.-F. L., Washenfelder, R. A., Notholt, J., Connor, B. J., Griffith, D. W. T., Sherlock, V., and Wennberg, P. O.: The total carbon column observing network, Philos. T. R. Soc. A, 369, 2087–2112, doi:10.1098/rsta.2010.0240, 2011. 8541, 8548

Yoshimura, K., Frankenberg, C., Lee, J., Kanamitsu, M., Worden, J., and Röckmann, T.: Comparison of an isotopic atmospheric general circulation model with new quasi-global satellite measurements of water vapor isotopologues, J. Geophys. Res.-Atmos., 116, D19118, doi:10.1029/2011JD016035, 2011. 8541, 8550, 8554, 8557

Zakharov, V. I., Imasu, R., Gribanov, K. G., Hoffmann, G., and Jouzel, J.: Latitudinal distribution of the deuterium to hydrogen ratio in the atmospheric water vapor retrieved from IMG/ADEOS data, Geophys. Res. Lett., 31, 12104, doi:10.1029/2004GL019433, 2004. 8541

AMTD
5, 8539–8578, 2012

Table 1. Statistics of the differences in fitted H_2O columns between our retrievals for two different windows in the 2.3 µm range using different line lists, and retrievals from TCCON's GFIT algorithm at 1.6 µm. Our updated spectroscopy leads to a clear reduction of the average reduced χ^2 of the fit residuals, $\langle\chi^2/\nu\rangle$, both compared to the original Jenouvrier et al. (2007) line list and HITRAN08. The precision σ, i.e. the standard deviation around the mean relative difference, shows no improvement. The median is most robust against the change in fitting window for the updated spectroscopy. The absolute value of the median (i.e. the bias) is not a very meaningful parameter as it depends on initial parameters and could easily be calibrated to zero. The last column shows the number of retrievals on which the statistics are based (if smaller than 50 then not all retrievals reached convergence).

Station	Line list	Window [cm^{-1}]	$\langle\chi^2/\nu\rangle$	σ	Median	N
Darwin	Updated	4174–4300	78.2	3.27 %	10.4 %	50
Darwin	Updated	4212–4248	71.0	3.32 %	9.98 %	50
Darwin	Jenouvrier	4174–4300	235	3.32 %	11.1 %	50
Darwin	Jenouvrier	4212–4248	108	3.17 %	13.5 %	50
Darwin	HITRAN08	4174–4300	242	2.90 %	5.22 %	50
Darwin	HITRAN08	4212–4248	307	2.56 %	1.43 %	50
Park Falls	Updated	4174–4300	63.6	4.05 %	7.63 %	50
Park Falls	Updated	4212–4248	77.9	4.25 %	7.10 %	46
Park Falls	Jenouvrier	4174–4300	168	3.83 %	9.72 %	50
Park Falls	Jenouvrier	4212–4248	98.1	3.90 %	11.3 %	46
Park Falls	HITRAN08	4174–4300	138	3.77 %	3.28 %	50
Park Falls	HITRAN08	4212–4248	147	4.33 %	1.42 %	47

AMTD
5, 8539–8578, 2012

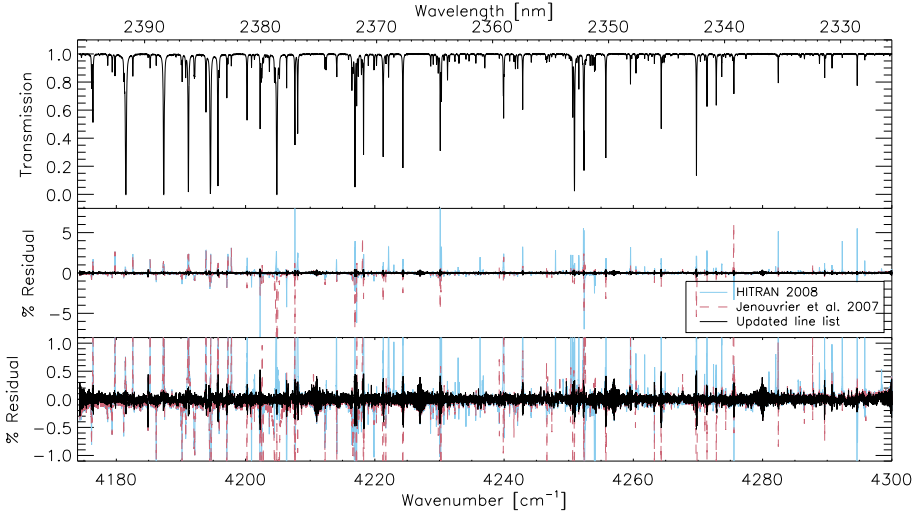

Fig. 1. Top: Laboratory spectrum of water vapour for $T = 293\,\mathrm{K}$, $P_{H_2O} = 4.04\,\mathrm{hPa}$ and $P_{air} = 333.6\,\mathrm{hPa}$, adopted from Jenouvrier et al. (2007, their run *j*). Middle: fit residuals (measured-modelled times 100) using HITRAN 2008 (blue), the original Jenouvrier et al. (2007) line list (red) and after fitting for the line parameters in this work (black). Bottom: close-up of the middle panel.

AMTD
5, 8539–8578, 2012

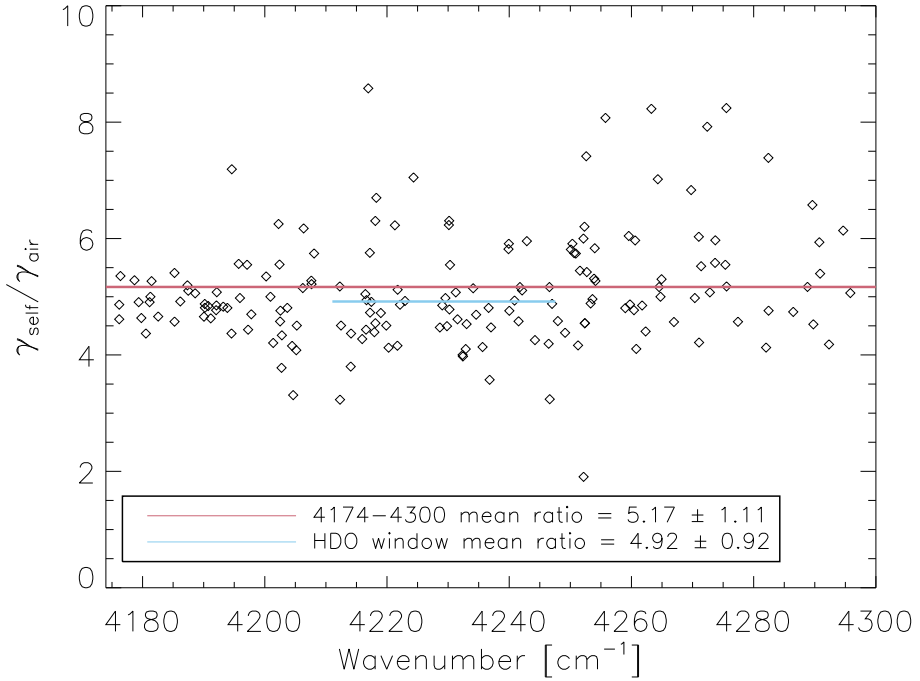

Fig. 2. Ratios between the self-broadened and air-broadened half-widths of the original Jenouvrier et al. (2007) spectroscopy. Plotted for the 174 lines with a line intensity stronger than 10^{-25} cm^{-1}(molecule cm^{-2})$^{-1}$. The red and blue lines indicate the mean ratio for the 4174–4300 cm^{-1} and the HDO retrieval window (4212–4248 cm^{-1}), respectively.

AMTD
5, 8539–8578, 2012

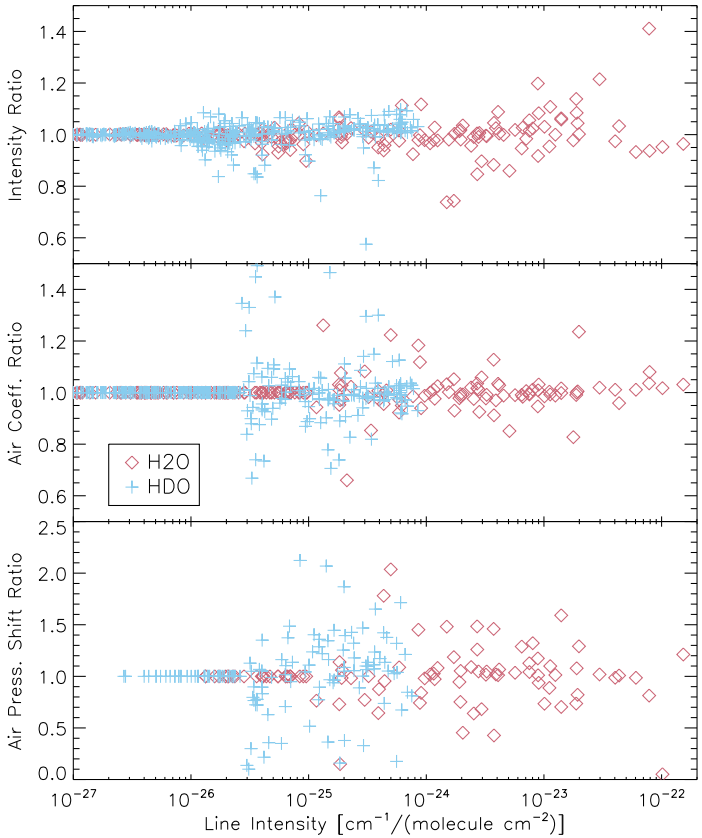

Fig. 3. Ratio of the updated line parameters over the original line parameters. Top: line intensities. Middle: air broadening coefficients. Bottom: air pressure shifts.

AMTD
5, 8539–8578, 2012

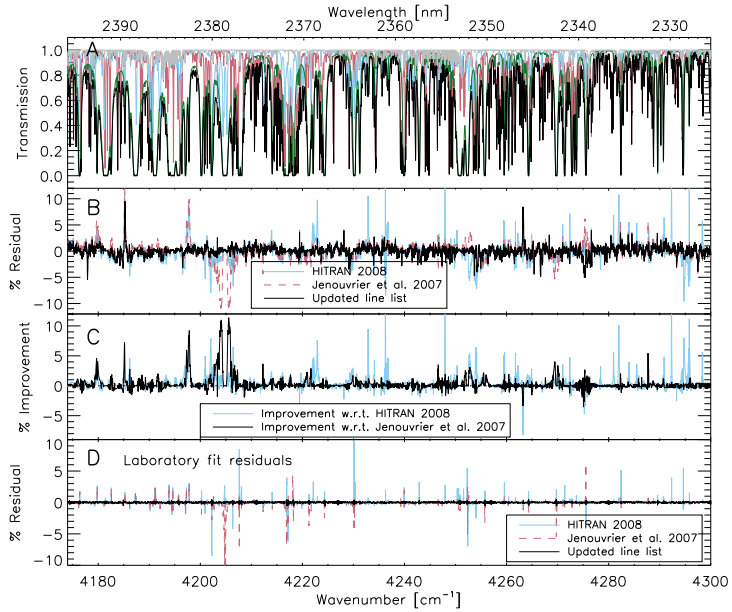

Fig. 4. Impact of the updated spectroscopy on the fit residuals of an FTS spectrum taken at Paramaribo. **(A)** Measured normalized transmission (black). The different colours show the contributions of all the modelled species (red: CH_4, green: H_2O, blue: HDO, grey: sun reference). **(B)** Residuals, plotted as 100×(spectrum-model) for a fit using HITRAN 2008 (blue), the original Jenouvrier et al. (2007) spectroscopy (red) and the updated spectroscopy from this work (black). **(C)** Difference between the absolute values of the residuals using HITRAN 2008 and this work (blue) and the original Jenouvrier et al. (2007) and this work (black). Positive values indicate improved residuals, while negative values indicate deteriorated residuals. The majority of the residuals improved w.r.t. HITRAN 2008 and Jenouvrier et al. (2007), while only a few residuals deteriorated. **(D)** The corresponding laboratory fit residuals of the water lines from Fig. 1.

AMTD
5, 8539–8578, 2012

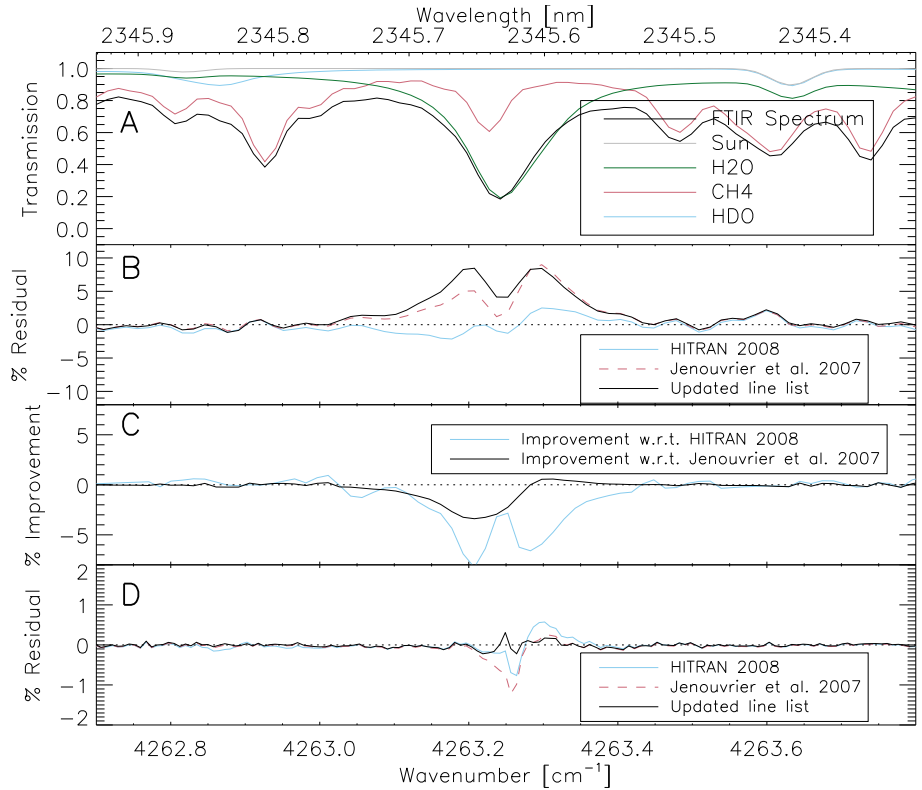

Fig. 5. Close-up of Fig. 4 around a line of which the residuals deteriorate. **(A)** Measured normalized transmission. The different colours show the contributions of all the modelled species. **(B)** Residuals. **(C)** Difference between the absolute values of the residuals. **(D)** The corresponding laboratory fit residuals.

AMTD
5, 8539–8578, 2012

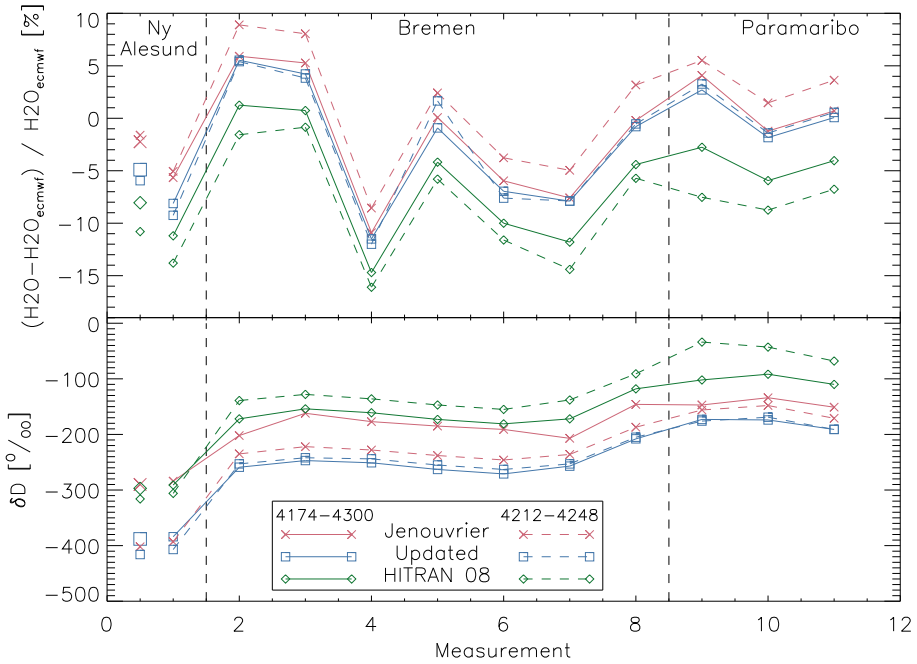

Fig. 6. The impact of the different line lists and retrieval windows on the H_2O column and δD from different ground-based FTS spectra. Solid and dashed lines are for the 4174–4300 cm^{-1} and 4212–4248 cm^{-1} window, respectively. Measurements for the different stations are separated by the vertical dashed lines (stations indicated at the top). Top: relative difference with the total column H_2O derived from ECMWF. For the Ny Ålesund retrieval we also compare with the total column derived from a radiosonde, indicated by the separated symbols on the left (large symbols for 4174–4300 cm^{-1} and small symbols for 4212–4248 cm^{-1}). Bottom: retrieved δD.

AMTD
5, 8539–8578, 2012

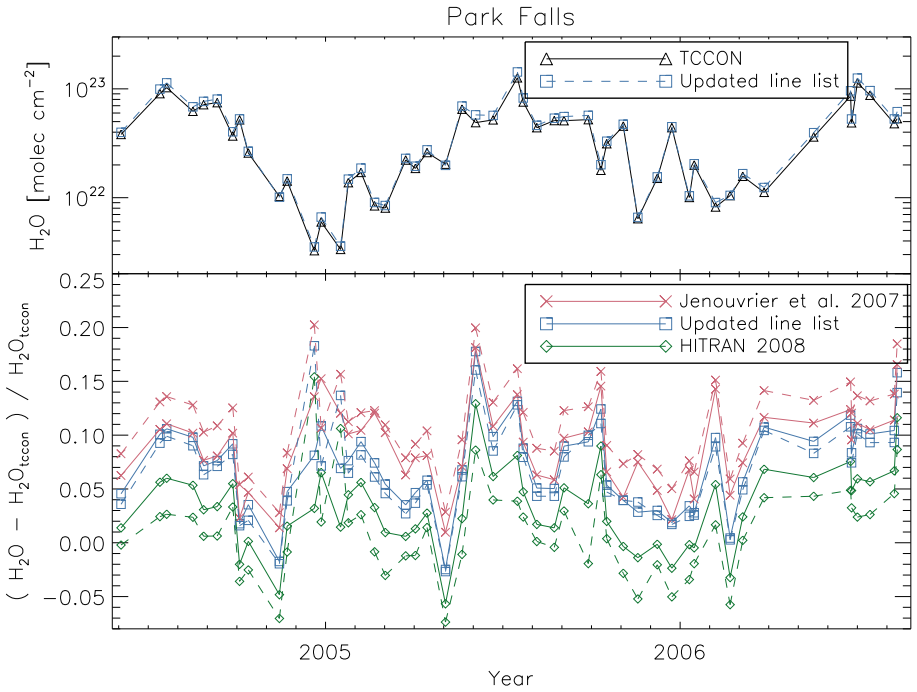

Fig. 7. H_2O FTS retrieval accuracy for Park Falls. Top: time series of the fitted H_2O columns using TCCON's GFIT algorithm at 1.6 µm, compared to using our updated line list in the 4174–4300 cm^{-1} range (2.3 µm). Bottom: time series of the relative differences with TCCON for all different line lists. Solid and dashed lines are for the 4174–4300 cm^{-1} and 4212–4248 cm^{-1} window, respectively.

AMTD
5, 8539–8578, 2012

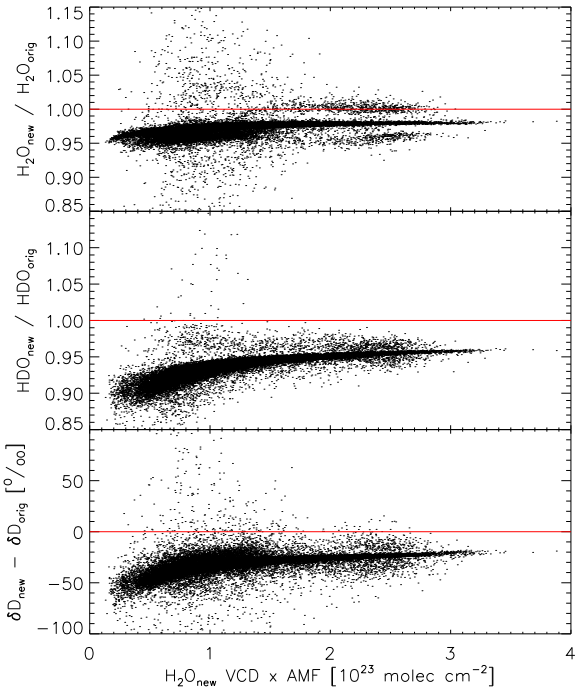

Fig. 8. Top: Ratio between all the retrieved vertical column densities (VCDs) for SCIAMACHY in June 2003 of H_2O using the updated spectroscopy ("new") and the original spectroscopy ("orig"). Plotted as a function of the H_2O VCD multiplied by the air mass factor (AMF), which is a good metric for the total amount of water vapour as seen by the detector. The updated spectroscopy leads to a reduction of the H_2O columns of ~ 2–5 % for the majority of the ground pixels. Middle: same for the retrieved HDO VCD. The updated spectroscopy leads to a reduction of the HDO columns of ~4–10 % for the majority of the ground pixels and the reduction increases for the driest columns. Bottom: Shift in δD corresponding to the top two panels. The updated spectroscopy leads to a negative shift of ~ 25 ‰ for the majority of the ground pixels and this shift becomes larger for the driest columns.

AMTD
5, 8539–8578, 2012

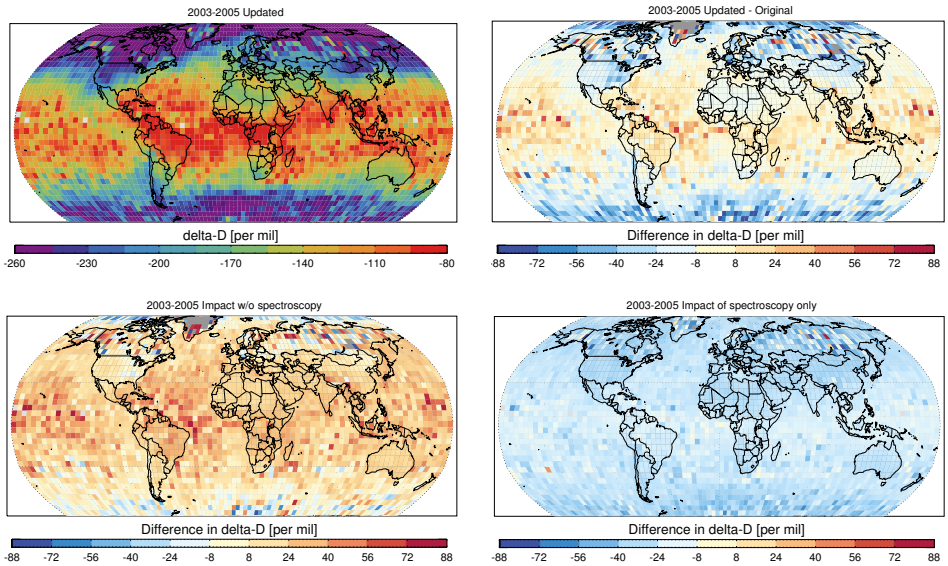

Fig. 9. Top left: updated 2003–2005 global average world map of δD. Top right: difference between the updated world map and the orignal world map from Frankenberg et al. (2009). Bottom left: impact on the world map solely caused by updates in the instrument calibration (the original spectroscopy was used). Bottom right: impact on the world map solely caused by the updated spectroscopy.

AMTD
5, 8539–8578, 2012

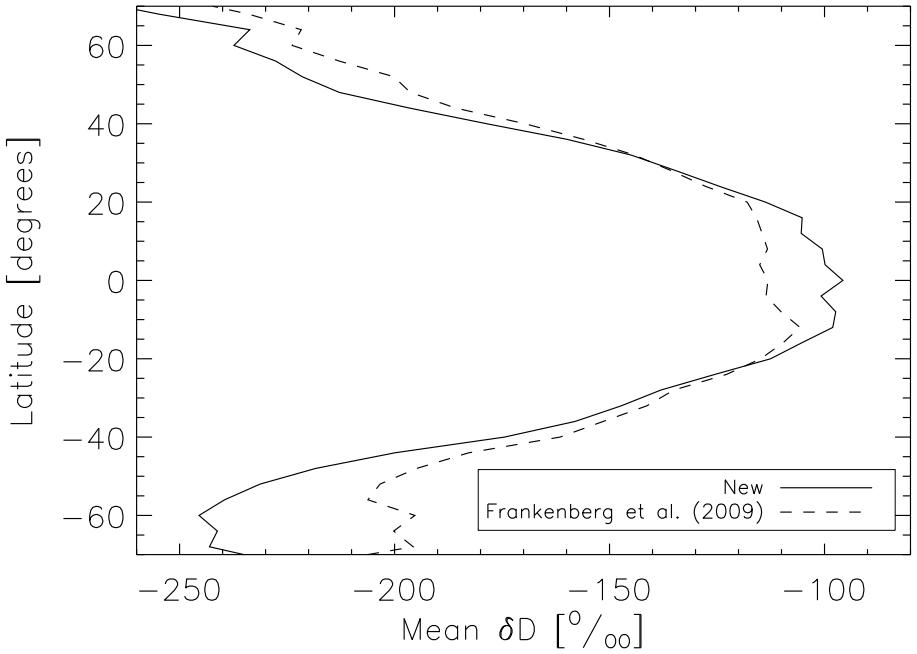

Fig. 10. Latitudinal gradient of δD of the new retrieval (including spectroscopic updates and new calibration software) compared to the results from Frankenberg et al. (2009).

AMTD
5, 8539–8578, 2012

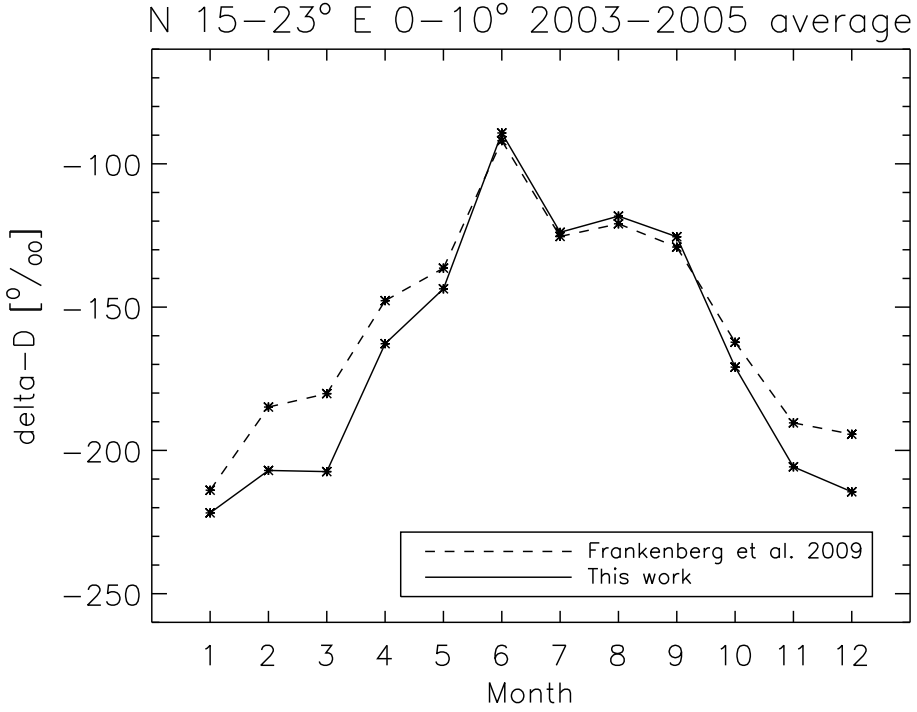

Fig. 11. Impact of the retrieval updates on the seasonality in the Sahel (following Frankenberg et al. (2009), both seasonalities have been shifted by −20 ‰).

AMTD
5, 8539–8578, 2012

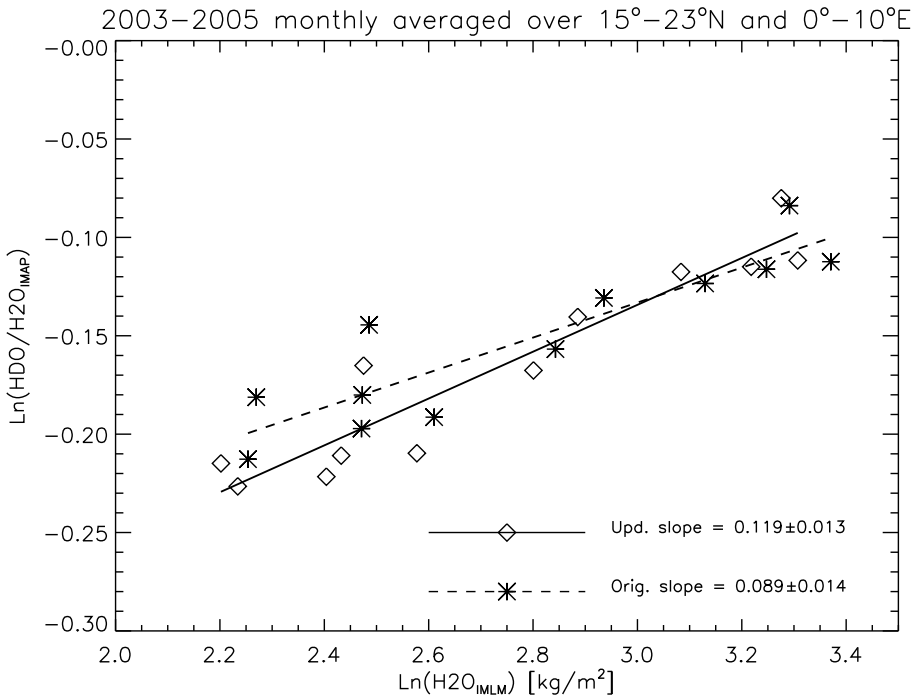

Fig. 12. Rayleigh-type plot for the region above the Sahel. Monthly averages were taken for the years 2003–2005. For the x-axis, H_2O retrievals from the IMLM algorithm of Schrijver et al. (2009) were used and matched with our retrievals of the HDO/H_2O ratio (y-axis). Comparing the original retrievals (stars and dashed line) with the updated retrievals (diamonds and solid line), we find that the updates lead to a steeper slope. The updated and original slope correspond to a fractionation temperature of 266 ± 7 K and 285 ± 10 K, respectively. For the updated retrievals the correlation coefficient increases from 0.90 to 0.95.

AMTD
5, 8539–8578, 2012

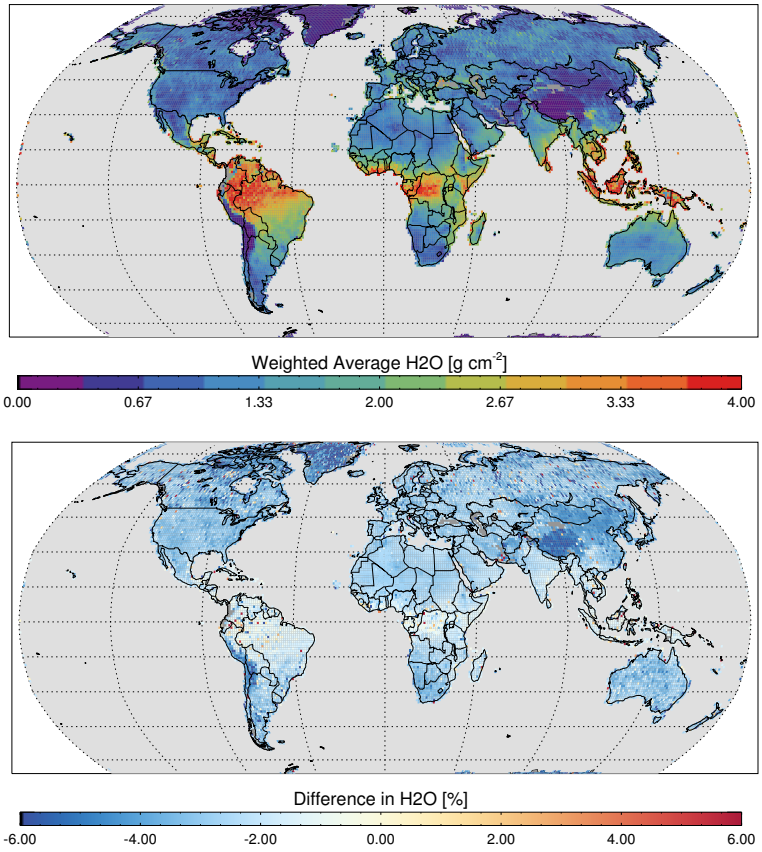

Fig. 13. Top: 2005–2007 weighted average of water vapour using the IMLM retrieval algorithm with the original Jenouvrier et al. (2007) line parameters. Bottom: relative differences ((new-original)/original) caused by the updated water spectroscopy.

AMTD
5, 8539–8578, 2012

Improved water vapour spectroscopy in the 4174–4300 cm^{-1} region

R. A. Scheepmaker et al.